Article

Data analytics-driven selection of die material in multimaterial co-extrusion of Ti-Mg alloys

Daniel Fernández *, Alvaro Rodríguez-Prieto and Ana María Camacho

[1] Department of Manufacturing Engineering, Universidad Nacional de Educación a Distancia (UNED), 28040 Madrid, Spain; alvaro.rodriguez@ind.uned.es (A.R-P.); amcamacho@ind.uned.es (A.M.C.)
* Correspondence: dfernande146@alumno.uned.es

Abstract: Selection of the most suitable material is one of the key decisions to be taken at the design stage of a manufacturing process. Traditional approaches as Ashby maps based on material properties are widely used in the industry. However, in the production of multimaterial components, the criteria for the selection can include antagonistic approaches. The aim of this work is the implementation of a methodology based on the results of process simulations for several materials and classify them by applying an advanced data analytics method based on Machine Learning (ML), in this case the Support Vector Regression (SVR) and Multi-Criteria Decision Making (MCDM) methodologies, specifically Multi-criteria Optimization and Compromise Solution (VIKOR) combined with Entropy weighting methods. In order to do this, a Finite Element Model (FEM) has been built to evaluate the extrusion force and the die wear in a multi-material co-extrusion process of bimetallic Ti6Al4V-AZ31B billets. After applying SVR and VIKOR combined with Entropy weighting methodologies, a comparison has been established based on the material selection and complexity of the methodology used, resulting that material chosen in both methodologies is very similar and MCDM method is easier to implement because there is no need of evaluate the error of the prediction model and the time for data preprocessing is less than the time needed in SVR. This new methodology is proven to be effective as alternative to the traditional approaches and aligned with the new trends in the industry based on simulation and data analytics.

Keywords: Data analytics, Methodologies**,** Multi-material; Co-extrusion; FEM; Machine Learning; SVR; MCDM.

Citation: Lastname, F.; Lastname, F.; Lastname, F. Title. *Mathematics* **2022**, *10*, x. https://doi.org/10.3390/xxxxx

Academic Editor: Firstname Lastname

Received: date
Accepted: date
Published: date

1. Introduction

In the recent years and with the raise of the Industry 4.0, simulation and data analytics methodologies have become more relevant due to their capacity of predict results and being more sustainable compared with the traditional approaches. The need of developing lighter materials in aerospace and automotive industry is increasing to improve the fuel efficiency reducing the environmental impact and increasing the payload to be carried out. Multi-material forming has become a solution because of the capacity to reduce the weight by joining dissimilar materials and also to customize the mechanical properties of the final part to fulfil with the in-service requirements.

Aluminium alloys and carbon fiber reinforced composites are widely used in aerospace industry; however, magnesium alloys have lower density and also good specific strength [1] therefore they could be a good alternative to reduce weight if it wasn´t for its poor corrosion resistance. Because of this, a multi-material component made of magnesium alloys combined titanium alloys, which have an excellent mechanical and physical-

chemical properties together with very good strength to weight ratio and superior corrosion resistance [2], could be the solution to manufacture lighter parts with good mechanical properties and without corrosion problems and thus, contribute to reduce the weight of the aircraft.

Within multi-material forming highlights co-extrusion process to obtain bimetallic billets composed of a cylindrical sleeve and core made of different materials. Some application cases of multi-material forming processes with these two alloys that can be highlighted are the ones performed by Fernández et al. [3, 4] who analysed the effect of the different co-extrusion process parameters by Finite Element Analysis (FEM) simulation using Analysis of Variance (ANOVA) to determine the most relevant ones and also investigated the effect of the selection die material on the co-extrusion process of bimetallic cylindrical billets made of magnesium alloy core and titanium alloy sleeve. Other interesting contributions are the ones performed by Negendanka et al. [5] who carried out a study about the diffusion layer formation under different die angle values in a Mg–core and Al–sleeve billet or Gall et al. [6], who studied the co-extrusion of bimetallic Al–Mg billets into hollow profiles by means of Finite Element Method (FEM) simulation together with experiments.

On the other hand, Machine Learning (ML) [7] has been gaining more relevance in the industry as preferred method to forecast results and anticipate problems [8] by means of algorithms based on statistical methods to detect patterns from data. Support Vector Machines (SVM) is one of the most popular supervised learning methods within ML. It was introduced by Vladimir Vapnik [9] in 1995 and its main applications are classification and regression analysis. For this last one is especially interesting the Support Vector Regression (SVR) module implemented within SVM to estimate discrete values and thus predict future results. Some examples of SVR applications in the industry are the prediction of the laser cutting process cost for AISI316L stainless steel [10], prediction of the cutting force and temperature in bone drilling [11], prediction of the drilling force drilling an internal hole in carbon-fiber-reinforced polymer (CFRP) [12] and applied to wear prediction it can be highlighted the research performed by Benkedjouh et al. [13].

Apart from ML, there are other approaches that allow to take decisions in situations where there are several requirements to fulfil in a complex environment and involving large number of variables. Multi-Criteria Decision Making (MCDM) methods based on multi objective optimization are applied to find the compromise solution to the problem. The first MCDM method was applied by Pareto in 1896 [14] with his famous 80/20 principle. Another example is Saaty in 1977 [15], who used multi-criteria models to solve problems with conflicting goals. Several MCDM methods have been developed and applied to support decision-making in different areas such as, manufacturing process selection [16], supply chain managing contract selection [17] and material selection [18]. In this research a combination of VIKOR [19] together with Entropy weighting methods [20, 21] has been chosen as MCDM methodology to establish the optimum die material selection, based on the results of the study performed by Fernández et al. [22] where different ARAS [23], TOPSIS [24], VIKOR and COPRAS [25] MCDM method were compared in conjunction with AHP [26], Standard Deviation [27] and Entropy weighting methods.

This study develops two methodologies, one based on SVR and the other applying Entropy weighting method together with MCDM VIKOR, for material selection of the die in a multi-material co-extrusion process to obtain bimetallic billets made of Ti6Al4V-AZ31B. Both methodologies and their results are compared to establish which one gives better results for the problem proposed.

2. Materials and Methods

2.1. Materials, Geometrical Dimensions and Process Parameters

In this study a bimetallic billet made of a Ti6Al4V titanium alloy sleeve and AZ31B magnesium alloy core during a co-extrusion process is analyzed.

Figure 1 shows the co-extrusion set up with process parameters and initial dimensions.

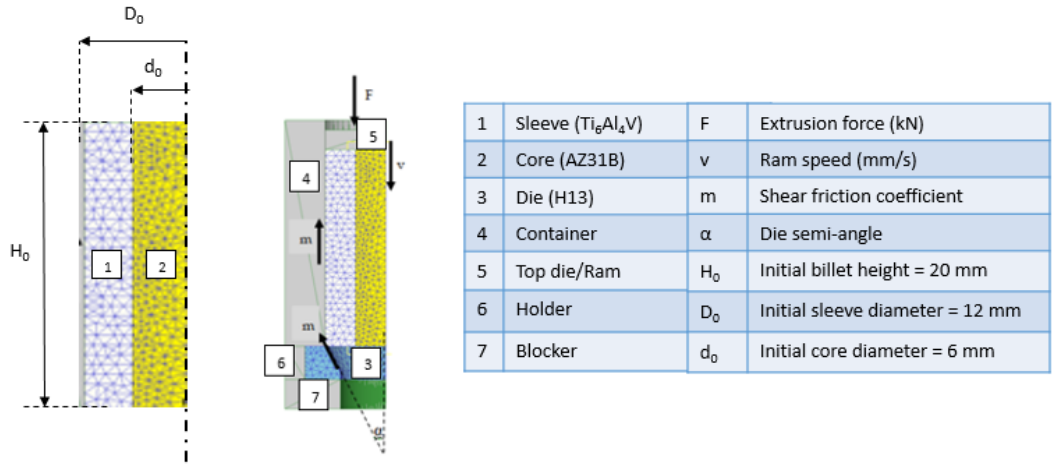

1	Sleeve (Ti_6Al_4V)	F	Extrusion force (kN)
2	Core (AZ31B)	v	Ram speed (mm/s)
3	Die (H13)	m	Shear friction coefficient
4	Container	α	Die semi-angle
5	Top die/Ram	H_0	Initial billet height = 20 mm
6	Holder	D_0	Initial sleeve diameter = 12 mm
7	Blocker	d_0	Initial core diameter = 6 mm

Figure 1. Co-extrusion set up with process parameters and initial billet dimensions

Main physical and mechanical properties for Ti6Al4V and AZ31B are shown in Table 1:

Table 1. Physical and mechanical properties of the titanium alloy Ti6Al4V and magnesium alloy AZ31B [28-29]

Property	Ti6Al4V	AZ31B
Density (g/cm³)	4.46	1.74
Tensile strength (MPa)	895	260
Yield strength (MPa)	828	200
Elastic modulus (GPa)	110	44.80
Poisson's ratio	0.31	0.35

Chemical compositions for Ti6Al4V and AZ31B are collected in Table 2 and Table 3 respectively:

Table 2. Chemical composition of titanium alloy Ti6Al4V [28]

Ti (wt.%)	Al (wt.%)	V (wt.%)	Fe (wt.%)	C (wt.%)	O (wt.%)	N (wt.%)	H (wt.%)
Bal.	5.5–6.5	3.5–4.5	0.25	0.08	0.13	0.040	0.012

Table 3. Chemical composition of magnesium alloy AZ31B [29]

Mg (wt.%)	Al (wt.%)	Zn (wt.%)	Mn (wt.%)	Si (wt.%)	Cu (wt.%)	Ca (wt.%)	Fe (wt.%)	Ni (wt.%)
97	2.5–3.5	0.6–1.4	0.20	0.1	0.05	0.04	0.005	0.005

The material candidates for the die are extracted from Daniel et al. [4] which chemical composition and physical and mechanical properties are shown in Table 4 and 5 respectively.

Table 4. Chemical composition of die steels [30-34].

Material	C (wt.%)	Mn (wt.%)	Si (wt.%)	Cr (wt.%)	Mo (wt.%)	Ni (wt.%)
AISI316	0.08	2	0.75	16–18	2–3	10–14
H13	0.32–0.45	0.2–0. 5	0.8–1.20	4.75–5.50	1.10–1.75	0.30 max
25CrMo4	0.22–0.29	0.60–0.90	0.10–0.40	0.90–1.20	0.15–0.30	-
AISI52100	0.1	0.45	0.26	1.51	0.06	3.39
AISI3310	0.99	0.39	0.16	1.4	-	1.4

Table 5. Physical and mechanical properties of die steels [35].

Property	AISI316	H13	25CrMo4	AISI52100	AISI3310
Density (g/cm^3)	8.03	7.78	7.85	7.83	7.81
Tensile strength (MPa)	550	1990	670	992	1866
Yield strength (MPa)	240	1650	435	579	1800
Elastic modulus (GPa)	210	210	205	200	210
Poisson's ratio	0.3	0.3	0.3	0.3	0.3

The extrusion process parameters evaluated during this research are the following:

- Process parameters: Ram speed (mm/s) and temperature (° C).
- Tooling parameters: Die semi-angle (°), shear friction factor, and extrusion ratio (A_0/A_f).
- Geometric parameters: Shape factor (H_0/D_0) and diameter ratio (D_0/d_0).

Where A_0 and A_f are the initial and final area of the cross-section of the billet, D_0 and d_0 the initial external diameter and internal diameter of the sleeve and H_0 the initial billet height.

2.2. Finite Element Modeling and Simulation preparation

Commercial software DEFORM3D© (v11.2) [36] was used to perform finite element simulations.

All parts were meshed with 7000 tetrahedral elements and due to the axial symmetry of the process, only one-quarter of the problem was modeled to reduce the computation time and to avoid heavy database files.

Contact condition among the objects of the simulation is defined as follows. Rigid and elastic objects were considered "masters" (those that deform) and the plastic objects were considered "slaves" (those that are deformed). In the case of the sleeve and core interaction, where both objects are plastic, the titanium alloy was defined as the "master" and the magnesium alloy was defined as the "slave". All materials were assumed to be isotropic throughout the process.

Heat transfer coefficient between sleeve and core and between sleeve and die was set to 11 N/(s·mm·°C), while between extrusion tooling elements and die was set to 5 N/(s·mm·°C). All the objects of the simulation have 0.02 N/(s·mm·°C) heat transfer coefficient with the air.

The exponential model defined by Wen-juan et al. [37] was used to define the behaviour of AZ31B while Johnson-Cook constitutive equations [38] were used for the definition of stress-strain curves for the Ti6Al4V.

2.2.1. *Tool wear model*

Archard's wear model is used to calculate the wear produced on the surface of the die [39–41]. This model is based on Equation (1):

$$W = \int K \cdot \frac{p^a \cdot v^b}{H^c} \cdot dt \quad (1)$$

Where K is the wear coefficient, P is the interface pressure, v is the sliding velocity between die and billet, H is the hardness and a, b and c are experimentally calibrated coefficients.

The commonly taken value for a and b is 1 while for c is 2 in the case of steel alloys. $K = 2 \times 10^{-5}$.

Taking into account Equation (1) the parameters to evaluate the wear are ram speed and friction as they can influence in the sliding velocity together with temperature because it has a direct influence in the stress-strain curves.

2.2.2. *FEM Model Validation*

FEM model was validated by using the semi-empirical model of Johnson, used by García et al. [42]. This model is typically used as reference in extrusion processes to establish an upper limit for the extrusion force. In order to apply the Johnson's model is necessary to obtain the average yield stress of each component in accordance with their volume fraction as it is described by Gisbert et al. [43]. The force obtained by FEM is in good agreement with the semi-empirical model results, being this last one an upper limit of the required forces, as expected, so the FE model can be considered validated.

2.3. Support Vector Regression

SVM works by finding a hyperplane in a high-dimensional space that best separates data into different classes. It aims to maximize the margin (the distance between the hyperplane and the nearest data points of each class) while minimizing classification errors. SVM can handle both linear and non-linear classification problems by using various kernel functions. Unlike SVM used for classification tasks, SVR seeks to find a hyperplane that best fits the data points in a continuous space.

SVR [44] gives the flexibility to define how much error is acceptable in our model and will find an appropriate line (or hyperplane in higher dimensions) to fit the data. Therefore, the goal of SVR is to find a function that approximates the relationship between the input variables and a continuous target variable, while minimizing the prediction error.

Another advantage of the SVR over the linear or logistic regression, is the possibility of using different kernel functions such as polynomial or radial ones that allow to transform the data into a higher dimensional space which make it suitable for non-linear problems.

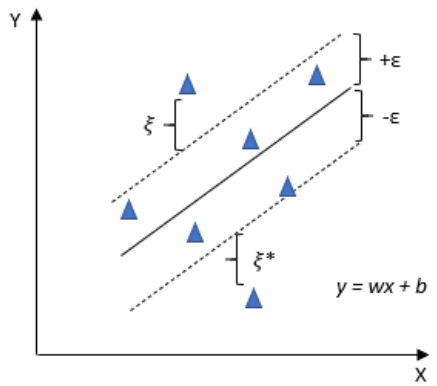

Figure 2. 2D hyperplane representation

As it was said before the idea is to minimize the Equation (2), taking into account the constraints of Equations (3), (4) and (5):

$$\frac{1}{2}\|w\|^2 + C\sum_{i=1}^{N}(\xi_i + \xi_i^*) \quad (2)$$

$$y_i - wx_i - b \leq \varepsilon + \xi_i \quad (3)$$

$$wx_i + b - y_i \leq \varepsilon + \xi_i^* \quad (4)$$

$$\xi_i, \xi_i^* \geq 0 \quad (5)$$

Where ε is the margin of error while ξ is the deviation from ε also called tolerance margin and w is the classification vector. C is known as the regularized parameter.

The prediction error can be calculated in different ways. One of the most representative is the determination factor (R^2) which shows the quality of correlation between the real measured data and the value predicted by Equation (6). A more precise correlation will be obtained for the value of the determination factor nearer to 100%.

$$R^2 = \frac{[\sum_{i=1}^{n}(\theta_i - \theta_i^{mean})(\hat{\theta}_i - \hat{\theta}_i^{mean})]^2}{[\sum_{i=1}^{n}(\theta_i - \theta_i^{mean})][\sum_{i=1}^{n}(\hat{\theta}_i - \hat{\theta}_i^{mean})]} \quad (6)$$

Where θ_i is the measurement data, $\hat{\theta}_i$ is the predicted magnitude in accordance with SVR, θ_i^{mean} is the mean of the measurement data and $\hat{\theta}_i^{mean}$ is the mean of the prediction.

2.4. *Entropy method*

Entropy method [21, 22] is classified within the category of objective weighting methods and it is applicable when the data of decision matrix are known. The entropy is a measure of randomness and disorder in the universe.

Starting with the decision matrix D the project outcomes p_{ij} are calculated by means of Equation (7).

$$\mathrm{D} = \begin{bmatrix} x_{11} & \cdots & x_{1n} \\ \vdots & \ddots & \vdots \\ x_{m1} & \cdots & x_{mn} \end{bmatrix}$$

$$p_{ij} = \frac{x_{ij}}{\sum_{i=0}^{m} x_{ij}} \quad (7)$$

Where n is the number of criteria and m the number of alternatives.

The entropy measure of project outcomes is obtained as it is shown in Equation (8).

$$E_j = -k * \sum_{i=1}^{m} p_{ij} * \ln(p_{ij}) \quad (8)$$

With $k = 1/ln\ (m)$.

Objective weight-based definition is given by Equation (9).

$$w_j = \frac{1 - E_j}{\sum_{j=1}^{n}(1 - E_j)} \quad (9)$$

2.5. *VIKOR method*

VIKOR method [45, 46] stands for *VIseKriterijumska Optimizacija I Kompromisno Resenje*, which means Multi-criteria Optimization and Compromise Solution.

This methodology is based on the concept that the compromise solution is the one which is at minimum distance for the ideal solution and at the same time at maximum distance for the anti-ideal solution.

One big different with SVM mehtod is that VIKOR does not need a calculation of the error because there is no prediction and therefore, there is nothing to compare with. Instead of that, VIKOR requests a validation step before declaring the compromise solution feasible by fulfilling the "acceptable advantage" and "acceptable stability in decision making" conditions.

Other advantages of using VIKOR method are the following:

- The ability to inmmediately recognize the proper alternative.
- Decreases the pairwise comparisons required.

After the criteria to be evaluated are defined the decision matrix (D) is built.

$$D = \begin{bmatrix} x_{11} & \cdots & x_{1n} \\ \vdots & \ddots & \vdots \\ x_{m1} & \cdots & x_{mn} \end{bmatrix}$$

At this point, the best f_b^* and worst f_b^- for each criteria rating values of the decision matrix.

$f_b^* = max\,(x_{ib}) \quad f_b^- = min\,(x_{ib})$ Whether the objective is to maximize the criteria.

$f_b^* = min\,(x_{ib}) \quad f_b^- = max\,(x_{ib})$ Whether the objective is to minimize the criteria.

Where $b = 1 \ldots m$ being m the number of criteria took into account and $i = 1 \ldots n$ and n is the number of the alternatives.

Utility measure (S_j) and Regret measure (R_j) are calculated according with Equations (10) and (11):

$$S_j = \sum_{b=1}^{m} W_b * \left[\frac{f_b^* - f_{ij}}{f_b^* - f_b^-}\right] \tag{10}$$

$$R_j = max\left[W_b * \left[\frac{f_b^* - f_{ij}}{f_b^* - f_b^-}\right]\right] \tag{11}$$

Where W_b are the weight values obtained in the case of this study after applied Entropy weighting methods explained above.

Index Q can be obtained by means of the Equation (12):

$$Q_a = \upsilon * \frac{S_j - S^*}{S^- - S^*} + (1 - \upsilon) * \frac{R_j - R^*}{R^- - R^*} \tag{12}$$

Where:

$$S^- = max\,(S_j)$$
$$S^* = min\,(S_j)$$
$$R^- = max\,(S_j)$$
$$R^* = min\,(S_j)$$

υ is a parameter which represents the type of voting used during the process ($\upsilon > 0.5$ means "vote by majority rule", $\upsilon = 0.5$ "vote by consensus" and $\upsilon < 0.5$ "with vote").

The lowest Q_a value indicates the best alternative solution and it can be recommended if the following conditions are satisfied:

The "acceptable advantage" condition means that $Q(a'') - Q(a') \geq DQ$. Being a'' the alternative in second position in the ranking list by Q_a and a' the first one. DQ is defined by Equation (13):

$$DQ = \frac{1}{(n-1)} \quad (13)$$

Where n is the number or alternatives.

Finally, the "Acceptable stability in decision making" condition implies that a' alternative must also be the best ranked in S_j and/or R_j. If one of the conditions is not fulfilled, then a set of compromise solutions is proposed.

2.5 Methodology

Two different methodologies have been proposed for the selection of the optimal die material in order to obtain the minimum extrusion force and die wear. The methodology steps are shown in Figure 3 flowchart.

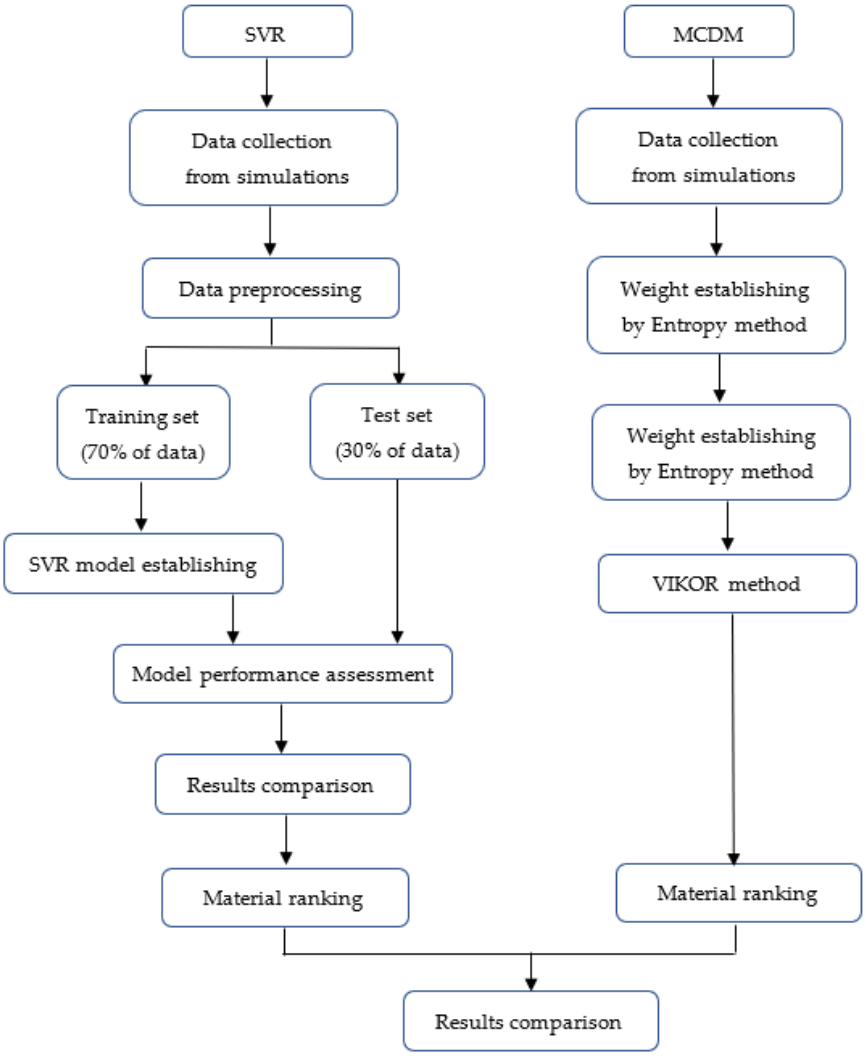

Figure 3. Methodology flowchart.

The criteria for the final results comparison are:

- Simplicity.
- Amount of data from simulations.

- Time consuming.

The prediction was carried out in Python software [47].

3. Results

In this paper a set of simulations of a multi-material co-extrusion process have been performed by using commercial software DEFORM3D© (v11.2) followed by application of two different methodologies to choose which is the best die material to obtain minimum extrusion force and minimum wear during the process. For the list of simulations carried out in the present work see Table A1 in the Appendix A.

3.1 SVR Methodology

As explained above the dataset is obtained from Table [6] and for each material and each parameter to be predicted, several dataframes were obtained by using "pandas" together with "sklearn" libraries.

Using "RFE" module for Regression Feature Selection from "sklearn.feature_selection" together with "SVR" module from "sklearn.svm", the influence of the process parameters are ranked in accordance with their influence in the extrusion force as it is shown in table 6.

Table 6. Process parameters ranking for extrusion force

Material	*Parameters*
AISI316	Extrusion ratio, friction, ram speed, core diameter, billet height, die semi-angle and temperature.
H13	Friction, extrusion ratio, core diameter, billet height, die semi-angle, ram speed and temperature.
25CrMo4	Friction, ram speed, billet height, core diameter, die semi-angle, temperature and extrusion ratio.
AISI52100	Friction, core diameter, die semi-angle, extrusion ratio, billet height, ram speed and temperature.
AISI3310	Ram speed, core diameter, friction, extrusion ratio, die semi-angle, billet height and temperature.

Taking into account these results, it can be said that friction is the most important process parameter while temperature is the less important one. This conclusion is in a good agreement with the findings obtained by Fernández et al. [3, 4] where a deeper analysis of the influence of each process parameter in the extrusion force was performed.

As there is not a clear pattern about the influence of each process parameters and this influence is clearly dependent on the die material, for the prediction model all the parameters will be implemented.

For the prediction model of the extrusion force, the dataframes for each material were split in two groups, one for training and one for testing using the "train_test_split" function from "sklearn.model_selection" module, being the test size 0.3.

After applying the "LinearRegression" function from "sklearn.linear_model" to build the prediction model using the training data and afterwards evaluate the model using the test data, the determination factor (R^2) for each material is shown in Table 7:

Table 7. Determination factor (R^2) for extrusion force linear regression model

Material	R^2
AISI316	0.91461
H13	0.92245
25CrMo4	0.70708
AISI52100	0.86922
AISI3310	0.91966

Figures 4 to 8 show the comparison between the simulation obtained values and the prediction ones.

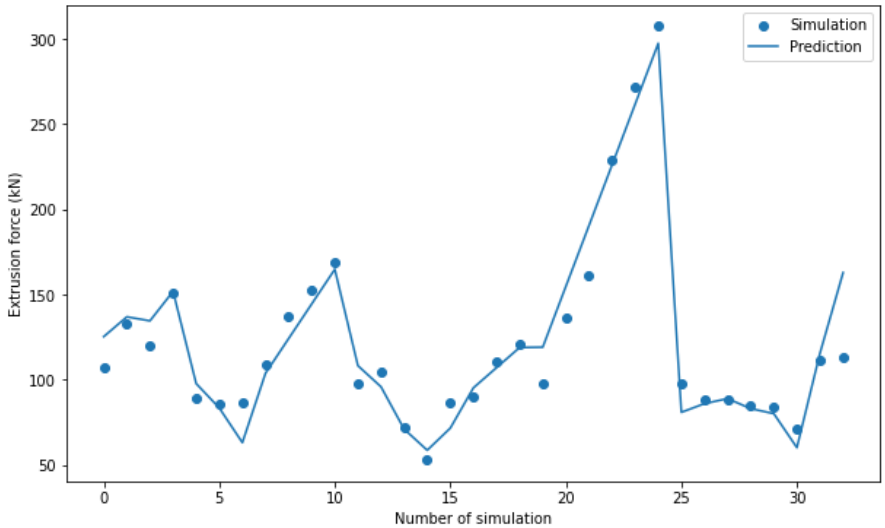

Figure 4. *AISI316 extrusion force prediction comparison*

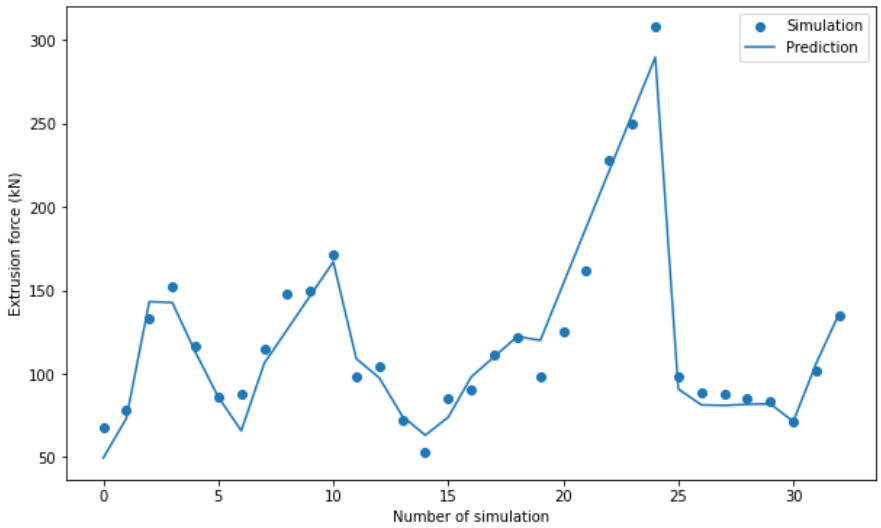

Figure 5. *H13 extrusion force prediction comparison*

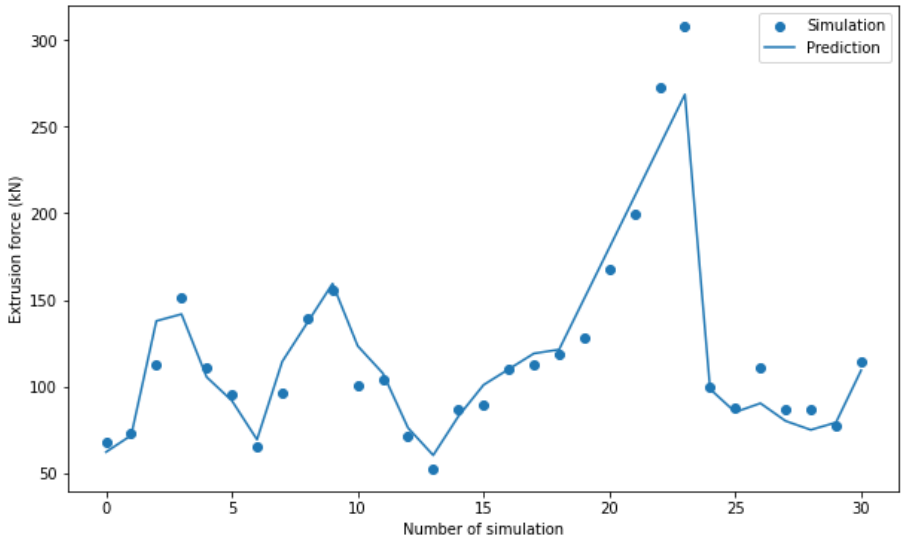

Figure 6. *25CrMo4 extrusion force prediction comparison*

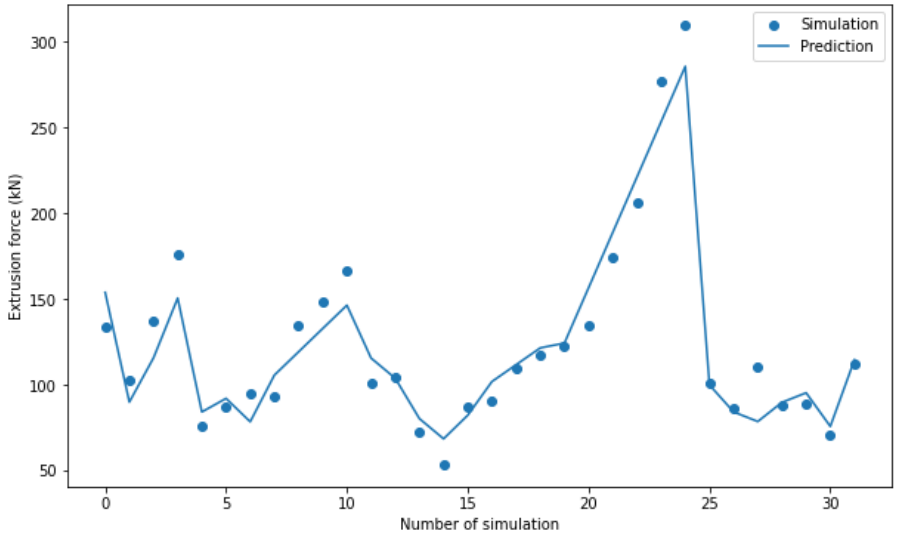

Figure 7. AISI52100 extrusion force prediction comparison

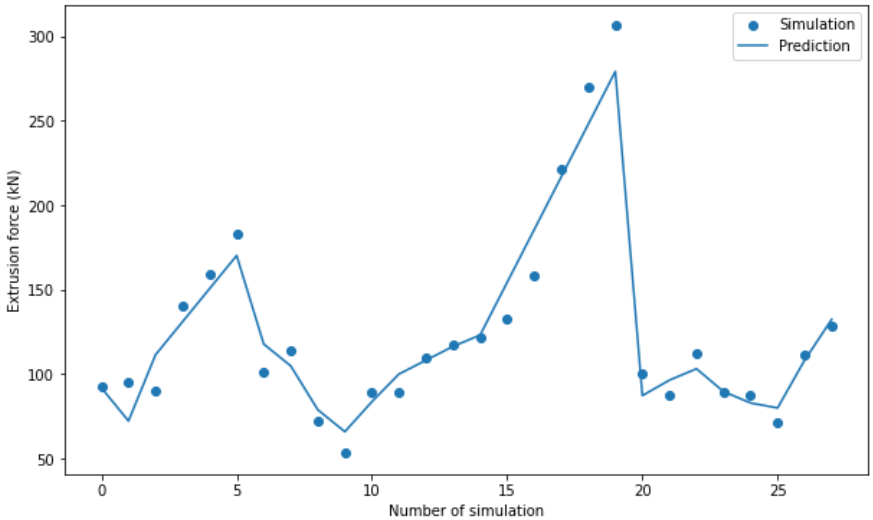

Figure 8. AISI3310 extrusion force prediction comparison

Using the prediction models for each die material a bigger number of results for the extrusion force can be compared without the need of performing more simulations. Table 8 show the ranking of the die materials as function of the times that their prediction value for the extrusion force is the lowest one.

Table 8. Die materials ranking as function of the lowest extrusion force produced.

Material	***Ranking***
AISI316	2
H13	2
25CrMo4	5
AISI52100	3
AISI3310	1

If there was only the minimum extrusion force as requirement for the die material election, AISI3310 would be the chosen one followed by AISI316 and H13 sharing the second position in the ranking.

The SVR methodology is now applied for the wear prediction with the following modification.

Due to the results variation is not possible to apply a linear model regression but a polynomial one. In order to do this is necessary to import "PolynomialFeatures" module from "sklearn.preprocessing" library to generate a new feature matrix consisting of all polynomial combinations of the features with degree less than or equal to the specified degree (in this case a 2 degree polynomial is used).

In Tables 9 and 10 are shown the process parameters ranking and the determination factor (R^2) for the wear model:

Table 9. Process parameters ranking for die wear

Material	*Parameters*
AISI316	Friction, ram speed and temperature.
H13	Friction, ram speed and temperature.
25CrMo4	Temperature, friction and ram speed.
AISI52100	Friction, temperature and ram speed.
AISI3310	Temperature, ram speed and friction.

This conclusion is in a good agreement with the findings obtained by Fernández et al. [4] where a deeper analysis of the influence of each process parameter in the die wear was performed.

Table 10. Determination factor (R^2) for extrusion force linear regression model

Material	R^2
AISI316	0.75695
H13	0.74873
25CrMo4	0.63223
AISI52100	0.80571
AISI3310	0.65881

The prediction model is not as accurate as the one for the extrusion force. This can be due to the number of simulations performed to obtain the wear distribution are lower than for the extrusion force because of Archad's wear model only takes into account temperature, friction and ram speed as it was mentioned in section 2.2.1.

Figures 9 to 13 show the comparison between the simulation obtained values and the prediction ones.

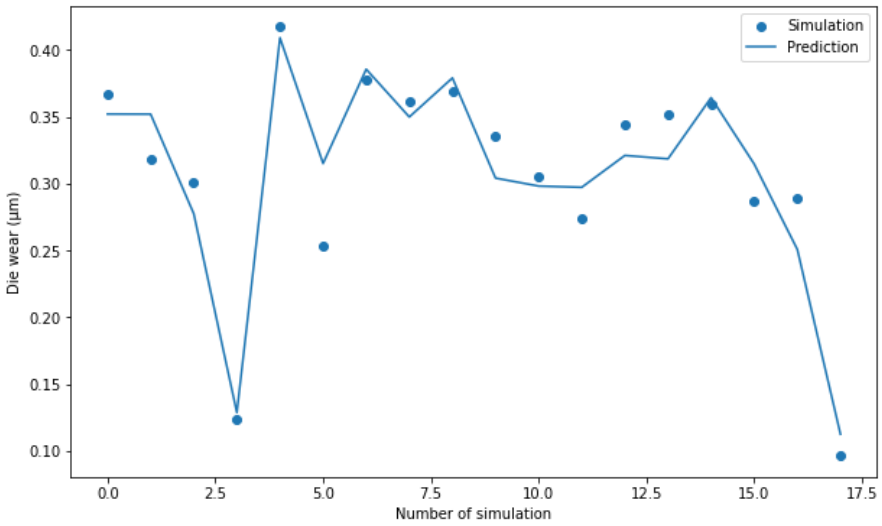

Figure 9. AISI316 die wear prediction comparison

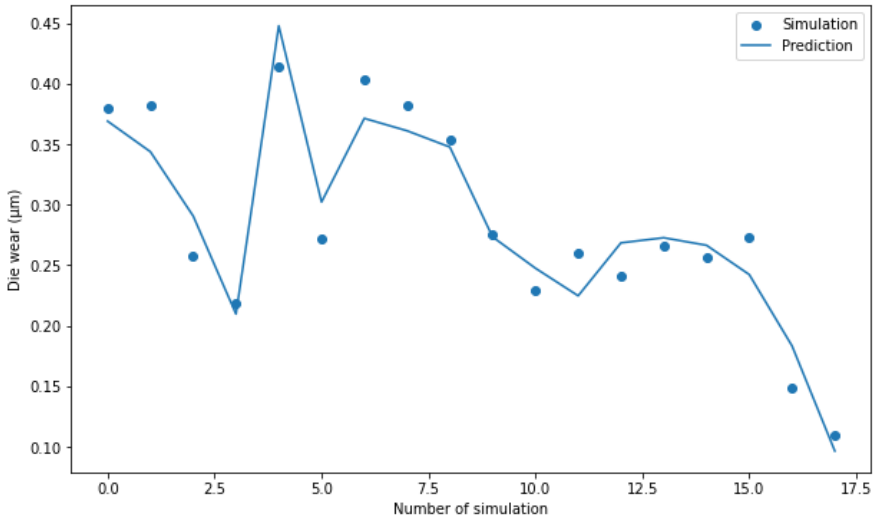

Figure 10. H13 die wear prediction comparison

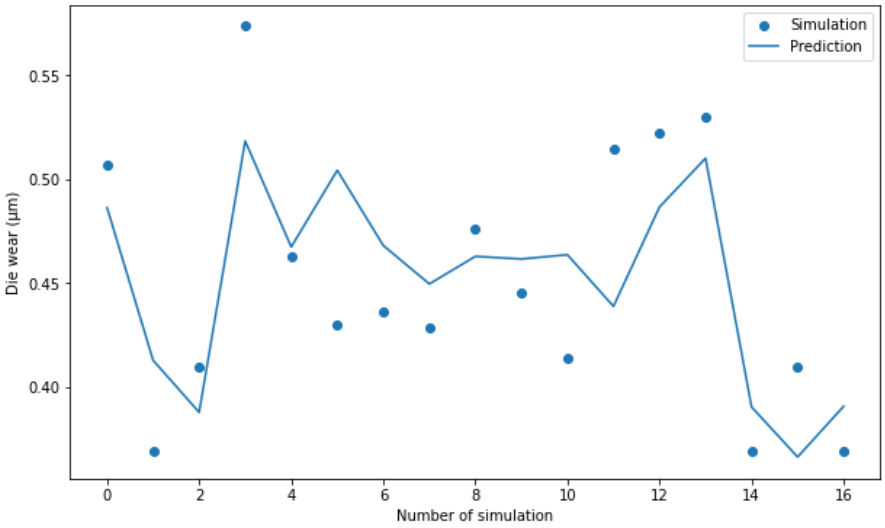

Figure 11. 25CrMo4 die wear prediction comparison

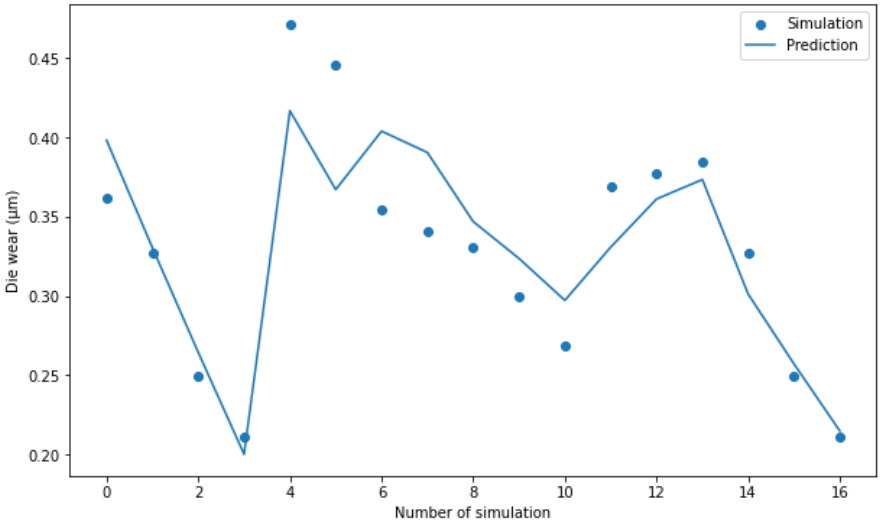

Figure 12. AISI52100 die wear prediction comparison

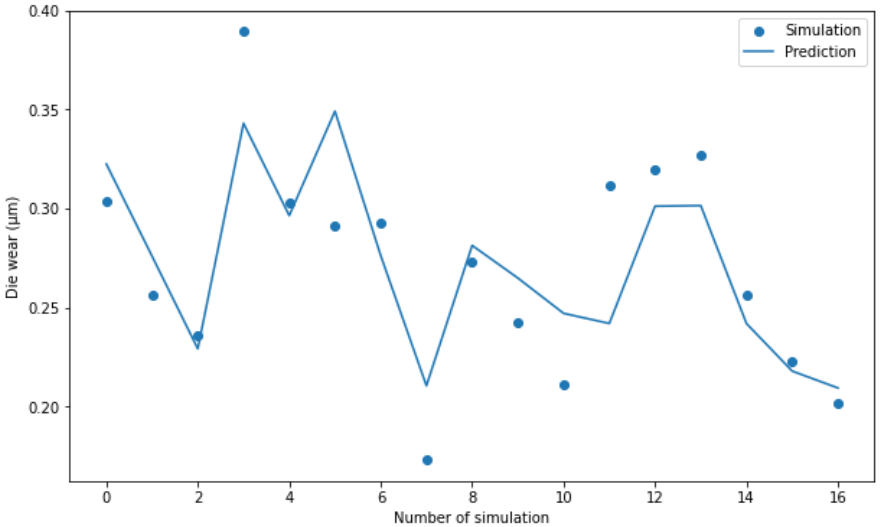

Figure 13. AISI3310 die wear prediction comparison

Table 11 show the ranking of the die materials as function of the times that their prediction value for the die wear is the lowest one.

Table 11. Die materials ranking as function of the minimum wear in the die produced.

Material	***Ranking***
AISI316	2
H13	3
25CrMo4	N/A
AISI52100	N/A
AISI3310	1

Finally, a crosscheck between Tables 8 and 11 is performed to rank the die material which fulfil better the minimum extrusion force and the minimum die wear as it can be seen in Table 12.

Table 12. Die materials ranking as function of the minimum extrusion force and the minimum die wear

Material	***Ranking***
AISI316	2
H13	3
25CrMo4	5
AISI52100	4
AISI3310	1

In both rankings AISI3310 is the best choice to reduce the extrusion force and die wear. AISI316 and H13 have the same position for the extrusion force but not for the die wear, this is the reason because in the final ranking AISI316 is positioned better than H13. The die materials that can be rejected as feasible option are AISI52100 and 25CrMo4.

3.2 MCDM Methodology

As explained in section 3. the dataset is obtained from Table A1. In the MCDM methodology the weights are calculated by means of Entropy method and afterwards VIKOR method is applied to classify the different materials based on criteria rating values decision.

For the Entropy method, the decision matrix D is obtained from the results for each simulation in Table A1 regarding extrusion force and die wear.

86.019	136.529	228.511	307.324	97.898	88.621	88.040	84.512	83.759	0.367	0.318	0.302	0.124	0.417	0.253	0.378	0.361	0.370
86.153	124.955	227.644	307.783	98.095	88.706	88.140	84.799	83.850	0.379	0.382	0.257	0.219	0.414	0.271	0.404	0.381	0.354
95.608	128.196	199.579	307.520	100.048	87.505	111.049	87.149	86.484	0.361	0.327	0.250	0.211	0.471	0.445	0.354	0.341	0.345
87.120	134.333	206.128	309.397	100.654	86.238	110.203	88.307	88.602	0.507	0.369	0.410	0.452	0.573	0.462	0.430	0.436	0.428
92.531	132.578	221.350	306.154	100.708	87.422	112.221	89.296	87.588	0.304	0.257	0.281	0.236	0.389	0.303	0.291	0.292	0.173

From D, the normalized matrix is obtained by means of Equation (7):

0.1923	0.2079	0.2110	0.1998	0.1968	0.2021	0.1727	0.1947	0.1947	0.1913	0.1925	0.2011	0.1000	0.1842	0.1459	0.2035	0.1993	0.2214
0.1926	0.1903	0.2102	0.2001	0.1972	0.2023	0.1729	0.1954	0.1949	0.1977	0.2311	0.1717	0.1764	0.1829	0.1563	0.2175	0.2105	0.2118
0.2137	0.1952	0.1842	0.1999	0.2011	0.1996	0.2179	0.2008	0.2010	0.1884	0.1978	0.1667	0.1701	0.2078	0.2568	0.1908	0.1881	0.2067
0.1947	0.2046	0.1903	0.2011	0.2024	0.1967	0.2162	0.2034	0.2059	0.2642	0.2233	0.2733	0.3639	0.2532	0.2665	0.2315	0.2407	0.2565
0.2068	0.2019	0.2043	0.1990	0.2025	0.1994	0.2202	0.2057	0.2036	0.1584	0.1553	0.1871	0.1897	0.1719	0.1744	0.1567	0.1614	0.1037

Then, the entropy array (Ej) is calculated by applying Equation (8):

Ej = [0.999418867 0.999681506 0.999085371 0.999996437 0.999952024 0.999966715 0.996102816 0.999852667 0.999839187 0.990960752 0.99430503 0.989129167 0.944884512 0.993690857 0.979914551 0.994771731 0.99470602 0.976990905]

The weights are presented in table 13:

Table 13. Entropy method weights

W. 1(%)	W. 2(%)	W. 3(%)	W. 4(%)	W. 5(%)	W. 6(%)	W. 7(%)	W. 8(%)	W. 9(%)	W. 10(%)	W. 11(%)	W. 12(%)	W. 13(%)	W. 14(%)	W. 15(%)	W. 16(%)	W. 17(%)	W. 18(%)
0.40	0.22	0.62	0	0.03	0.02	2.66	0.10	0.11	6.16	3.88	7.41	37.56	4.30	13.69	3.56	3.61	15.68

In VIKOR the best f_b^* and worst f_b^- values for each criterion are obtained directly from decision matrix D.

	86.019	136.529	228.511	307.324	97.898	88.621	88.040	84.512	83.759	0.367	0.318	0.302	0.124	0.417	0.253	0.378	0.361	0.370
	86.153	124.955	227.644	307.783	98.095	88.706	88.140	84.799	83.850	0.379	0.382	0.257	0.219	0.414	0.271	0.404	0.381	0.354
	95.608	128.196	199.579	307.520	100.048	87.505	111.049	87.149	86.484	0.361	0.327	0.250	0.211	0.471	0.445	0.354	0.341	0.345
	87.120	134.333	206.128	309.397	100.654	86.238	110.203	88.307	88.602	0.507	0.369	0.410	0.452	0.573	0.462	0.430	0.436	0.428
	92.531	132.578	221.350	306.154	100.708	87.422	112.221	89.296	87.588	0.304	0.257	0.281	0.236	0.389	0.303	0.291	0.292	0.173
	447.431	656.591	1083.212	1538.178	497.402	438.492	509.653	434.063	430.283	1.918	1.652	1.499	1.242	2.265	1.735	1.856	1.812	1.669
f_i*	86.019	124.955	199.579	306.154	97.898	86.238	88.040	84.512	83.759	0.304	0.257	0.250	0.124	0.389	0.253	0.291	0.292	0.173
f_i-	95.608	136.529	228.511	309.397	100.708	88.706	112.221	89.296	88.602	0.507	0.382	0.410	0.452	0.573	0.462	0.430	0.436	0.428

Utility measure (S_j) and Regret measure (R_j) are obtained:

	$\mathbf{S_j}$		$\mathbf{R_i}$
	0.23758265		0.12075866
	0.36022622		0.11092085
	0.44932592		0.1258087
	0.98459134		0.37557176
	0.21183731		0.12764252
$\mathbf{S}^*$	0.21183731	$\mathbf{R}^*$	0.11092085
$\mathbf{S}^-$	0.98459134	$\mathbf{R}^-$	0.37557176

Using the values S^*, S^-, R^* and R^- together with the assumption of vote by consensus ($\upsilon = 0.5$), the index Q is calculated:

	Q_i
AISI3310	0.03524455
H13	0.09601303
AISI52100	0.18179111
25CrMo4	1
AISI3310	0.03159193

In VIKOR the index *Q* is ranked from the lowest to the highest value, therefore the best material to obtain minimum extrusion force and minimum die wear is AISI3310. But before recommending this material as best compromise solution the conditions of "Acceptable advantages" and "Acceptable stability in decision making" have to be fulfilled.

In this case DQ = 0.25 according with Equation (13).

Q(2) – Q(1) = 0.0365261
Q(3) – Q(1) = 0.0644211
Q(4) – Q(1) = 0.15019917
Q(5) – Q(1) = 0.96840807 > DQ
Q(1) = *S**

As only the second condition is fulfilled, a set of compromise solution is presented and ranked in Table 14.

Table 14. Die materials VIKOR ranking

Material	Ranking
AISI316	2
H13	3
25CrMo4	4
AISI52100	5
AISI3310	1

4. Discussion

In this paper two methodologies are proposed to choose the best material for the die in a multi-material coextrusion process, taking into account that the process has to fulfil the requirements of minimum extrusion force and minimum die wear.

The first methodology proposed is the SVR based on SVM. The main advantage is the prediction model obtained during the process which allows the engineers to know the outcomes when varying the process parameters. On the other hand, the disadvantages are the number of simulations needed to obtain a good prediction model and depending on the results of those simulations the complexity to obtain the prediction model can be very high.

MCDM methodology allows to select the best die material with a smaller number of simulations than the SVR one and without considering the accuracy or complexity of prediction models. Also, it is less time consuming because Entropy and VIKOR methods can be applied directly to the data and there is no need to have knowledge in programming languages like Python.

The results for the top three materials selected are the same independently of the methodology applied. Therefore, if there is no need to obtain a prediction model to forecast results by applying other values to the parameters, the die material selection methodology recommended is MCDM one due to its simplicity and time saving to implement it because there is no need of data preprocessing, neither programming or statistical knowledge to interpretate the results of the model. In addition, MCDM is more scalable due to the fact that SVM needs to re-evaluate the model with the new data to ensure the adherence to the results while the prediction error is not increased.

Finally, for future research it would be interested a comparison among different machine learning methods to obtain a more robust prediction model not only for the wear but also for other parameters such as damage factor, mean stresses, microstructure resultant and so on.

Appendix A.

Table A1. List of simulations performed by DEFORM3D© (v11.2)

Simulation	Material	Ram speed (mm/s)	Core diameter (mm)	Billet Height (H)	Temperature (^{0} C)	Friction	Die semi-angle (^{0})	Extrusion Ratio
1	AISI316	2	5	20	200	0.2	30	1.78
2	AISI316	2	6	15	100	0.2	30	2.25
3	AISI316	2	7	25	100	0.3	30	1.44
4	AISI316	3	6	15	200	0.3	15	2.25
5	AISI316	3	7	15	300	0.2	45	1.44
6	AISI316	2	6	20	200	0.1	30	1.78
7	AISI316	2	6	20	200	0.1	15	1.78
8	AISI316	2	6	20	200	0.1	45	1.78
9	AISI316	2	6	20	200	0.1	60	1.78
10	AISI316	2	6	20	200	0.1	75	1.78
11	AISI316	2	6	20	200	0.1	90	1.78
12	AISI316	2	2	20	200	0.1	30	1.78
13	AISI316	2	4	20	200	0.1	30	1.78
14	AISI316	2	8	20	200	0.1	30	1.78
15	AISI316	2	10	20	200	0.1	30	1.78
16	AISI316	2	6	15	200	0.1	30	1.78
17	AISI316	2	6	25	200	0.1	30	1.78
18	AISI316	2	6	30	200	0.1	30	1.78
19	AISI316	2	6	35	200	0.1	30	1.78
20	AISI316	2	6	20	200	0.2	30	1.78
21	AISI316	2	6	20	200	0.3	30	1.78
22	AISI316	2	6	20	200	0.4	30	1.78
23	AISI316	2	6	20	200	0.5	30	1.78
24	AISI316	2	6	20	200	0.6	30	1.78
25	AISI316	2	6	20	200	0.7	30	1.78
26	AISI316	2	6	20	100	0.1	30	1.78

27	AISI316	2	6	20	300	0.1	30	1.78
28	AISI316	1	6	20	300	0.1	30	1.78
29	AISI316	3	6	20	300	0.1	30	1.78
30	AISI316	4	6	20	300	0.1	30	1.78
31	AISI316	2	6	20	200	0.1	30	1.44
32	AISI316	2	6	20	200	0.1	30	2.25
33	AISI316	2	6	20	200	0.1	30	2.94
34	H13	2	5	15	100	0.1	15	1.44
35	H13	2	6	25	300	0.1	15	1.78
36	H13	3	5	15	300	0.3	30	1.78
37	H13	3	6	25	100	0.2	45	1.44
38	H13	3	7	25	200	0.1	30	2.25
39	H13	2	6	20	200	0.1	30	1.78
40	H13	2	6	20	200	0.1	15	1.78
41	H13	2	6	20	200	0.1	45	1.78
42	H13	2	6	20	200	0.1	60	1.78
43	H13	2	6	20	200	0.1	75	1.78
44	H13	2	6	20	200	0.1	90	1.78
45	H13	2	2	20	200	0.1	30	1.78
46	H13	2	4	20	200	0.1	30	1.78
47	H13	2	8	20	200	0.1	30	1.78
48	H13	2	10	20	200	0.1	30	1.78
49	H13	2	6	15	200	0.1	30	1.78
50	H13	2	6	25	200	0.1	30	1.78
51	H13	2	6	30	200	0.1	30	1.78
52	H13	2	6	35	200	0.1	30	1.78
53	H13	2	6	20	200	0.2	30	1.78
54	H13	2	6	20	200	0.3	30	1.78
55	H13	2	6	20	200	0.4	30	1.78
56	H13	2	6	20	200	0.5	30	1.78
57	H13	2	6	20	200	0.6	30	1.78
58	H13	2	6	20	200	0.7	30	1.78
59	H13	2	6	20	100	0.1	30	1.78
60	H13	2	6	20	300	0.1	30	1.78
61	H13	1	6	20	300	0.1	30	1.78
62	H13	3	6	20	300	0.1	30	1.78
63	H13	4	6	20	300	0.1	30	1.78
64	H13	2	6	20	200	0.1	30	1.44
65	H13	2	6	20	200	0.1	30	2.25
66	H13	2	6	20	200	0.1	30	2.94
67	AISI52100	2	5	15	100	0.1	15	1.44
68	AISI52100	2	6	25	300	0.1	15	1.78

69	AISI52100	3	5	15	300	0.3	30	1.78
70	AISI52100	3	6	25	100	0.2	45	1.44
71	AISI52100	3	7	25	200	0.1	30	2.25
72	AISI52100	2	6	20	200	0.1	30	1.78
73	AISI52100	2	6	20	200	0.1	15	1.78
74	AISI52100	2	6	20	200	0.1	45	1.78
75	AISI52100	2	6	20	200	0.1	60	1.78
76	AISI52100	2	6	20	200	0.1	75	1.78
77	AISI52100	2	2	20	200	0.1	30	1.78
78	AISI52100	2	4	20	200	0.1	30	1.78
79	AISI52100	2	8	20	200	0.1	30	1.78
80	AISI52100	2	10	20	200	0.1	30	1.78
81	AISI52100	2	6	15	200	0.1	30	1.78
82	AISI52100	2	6	25	200	0.1	30	1.78
83	AISI52100	2	6	30	200	0.1	30	1.78
84	AISI52100	2	6	35	200	0.1	30	1.78
85	AISI52100	2	6	20	200	0.2	30	1.78
86	AISI52100	2	6	20	200	0.3	30	1.78
87	AISI52100	2	6	20	200	0.4	30	1.78
88	AISI52100	2	6	20	200	0.5	30	1.78
89	AISI52100	2	6	20	200	0.6	30	1.78
90	AISI52100	2	6	20	200	0.7	30	1.78
91	AISI52100	2	6	20	100	0.1	30	1.78
92	AISI52100	2	6	20	300	0.1	30	1.78
93	AISI52100	1	6	20	300	0.1	30	1.78
94	AISI52100	3	6	20	300	0.1	30	1.78
95	AISI52100	4	6	20	300	0.1	30	1.78
96	AISI52100	2	6	20	200	0.1	30	1.44
97	AISI52100	2	6	20	200	0.1	30	2.25
98	25CrMo4	2	6	20	200	0.3	45	1.44
99	25CrMo4	2	7	15	200	0.1	45	1.78
100	25CrMo4	3	5	25	200	0.2	15	1.44
101	25CrMo4	3	7	20	100	0.3	15	1.78
102	25CrMo4	2	6	20	300	0.1	30	1.78
103	25CrMo4	2	6	20	200	0.1	30	1.78
104	25CrMo4	2	6	20	200	0.1	15	1.78
105	25CrMo4	2	6	20	200	0.1	45	1.78
106	25CrMo4	2	6	20	200	0.1	60	1.78
107	25CrMo4	2	6	20	200	0.1	75	1.78
108	25CrMo4	2	6	20	200	0.1	90	1.78
109	25CrMo4	2	2	20	200	0.1	30	1.78
110	25CrMo4	2	4	20	200	0.1	30	1.78

111	25CrMo4	2	8	20	200	0.1	30	1.78
112	25CrMo4	2	10	20	200	0.1	30	1.78
113	25CrMo4	2	6	15	200	0.1	30	1.78
114	25CrMo4	2	6	25	200	0.1	30	1.78
115	25CrMo4	2	6	30	200	0.1	30	1.78
116	25CrMo4	2	6	35	200	0.1	30	1.78
117	25CrMo4	2	6	20	200	0.2	30	1.78
118	25CrMo4	2	6	20	200	0.3	30	1.78
119	25CrMo4	2	6	20	200	0.4	30	1.78
120	25CrMo4	2	6	20	200	0.5	30	1.78
121	25CrMo4	2	6	20	200	0.6	30	1.78
122	25CrMo4	2	6	20	200	0.7	30	1.78
123	25CrMo4	2	6	20	100	0.1	30	1.78
124	25CrMo4	2	6	20	300	0.1	30	1.78
125	25CrMo4	1	6	20	300	0.1	30	1.78
126	25CrMo4	3	6	20	300	0.1	30	1.78
127	25CrMo4	4	6	20	300	0.1	30	1.78
128	25CrMo4	2	6	20	200	0.1	30	1.44
129	25CrMo4	2	6	20	200	0.1	30	2.25
130	AISI3310	2	6	20	200	0.1	30	1.78
131	AISI3310	2	6	20	200	0.1	15	1.78
132	AISI3310	2	6	20	200	0.1	45	1.78
133	AISI3310	2	6	20	200	0.1	60	1.78
134	AISI3310	2	6	20	200	0.1	75	1.78
135	AISI3310	2	6	20	200	0.1	90	1.78
136	AISI3310	2	2	20	200	0.1	30	1.78
137	AISI3310	2	4	20	200	0.1	30	1.78
138	AISI3310	2	8	20	200	0.1	30	1.78
139	AISI3310	2	10	20	200	0.1	30	1.78
140	AISI3310	2	6	15	200	0.1	30	1.78
141	AISI3310	2	6	25	200	0.1	30	1.78
142	AISI3310	2	6	30	200	0.1	30	1.78
143	AISI3310	2	6	35	200	0.1	30	1.78
144	AISI3310	2	6	20	200	0.2	30	1.78
145	AISI3310	2	6	20	200	0.3	30	1.78
146	AISI3310	2	6	20	200	0.4	30	1.78
147	AISI3310	2	6	20	200	0.5	30	1.78
148	AISI3310	2	6	20	200	0.6	30	1.78
149	AISI3310	2	6	20	200	0.7	30	1.78
150	AISI3310	2	6	20	100	0.1	30	1.78
151	AISI3310	2	6	20	300	0.1	30	1.78
152	AISI3310	1	6	20	300	0.1	30	1.78

153	AISI3310	3	6	20	300	0.1	30	1.78
154	AISI3310	4	6	20	300	0.1	30	1.78
155	AISI3310	2	6	20	200	0.1	30	1.44
156	AISI3310	2	6	20	200	0.1	30	2.25
157	AISI3310	2	6	20	200	0.1	30	2.94

Author Contributions: Conceptualization, D.F., A.R.-P., and A.M.C.; methodology, D.F.; formal analysis, D.F., A.R.-P., and A.M.C.; investigation, D.F., A.R.-P., and A.M.C.; resources, A.R.-P. and A.M.C.; writing—original draft preparation, D.F.; writing—review and editing, A.R.-P. and A.M.C.; supervision, A.R.-P. and A.M.C.; project administration, A.R.-P. and A.M.C.; funding acquisition, A.R.-P. and A.M.C. All authors read and agreed to the published version of the manuscript.

Funding: This research was funded within the framework of the "Doctorate Program in Industrial Technologies" of the UNED and it has been funded by the project 2021V/-TAJOV/006 (awarded in the UNED Research Projects call named "Young Talents 2021").

Data Availability Statement: The raw/processed data required to reproduce these findings cannot be shared at this time as the data also forms part of an ongoing study.

Acknowledgments: We would like to extend our acknowledgement to the Research Group of the UNED "Industrial Production and Manufacturing Engineering (IPME)" and the Industrial Research Group "Advanced Failure Prognosis for Engineering Applications".

Conflicts of Interest: The authors declare no conflict of interest. The funders had no role in the design of the study; in the collection, analyses, or interpretation of data; in the writing of the manuscript; or in the decision to publish the results.

References

1. Sheng, L. Y., Du, B. N., Hu, Z. Y., Qiao, Y. X., Xiao, Z. P., Wang, B. J., Xu, D. K., Zheng, Y. F. & Xi, T. F. Effects of annealing treatment on microstructure and tensile behaviour of the Mg-Zn-Y-Nd alloy. *Journal of Magnesium Alloys* **2020**, 8, pp.601–613.
2. Bermudo, C., Andersson, T., Svensson, D., Trujillo, F. J., Martín-Béjar, S. & Sevilla, L. Modeling of the fracture energy on the finite element simulation in Ti_6Al_4V alloy machining. *Scientific Reports* **2021**, 11**,** 18490.
3. Fernández, D.; Rodríguez-Prieto, A.; Camacho, A.M. Effect of Process Parameters and Definition of Favorable Conditions in Multi-material Extrusion of Bimetallic AZ31B-Ti6Al4V Billets. Appl. Sci. 2020, 10, 8048.
4. Fernández, D.; Rodríguez-Prieto, A.; Camacho, A.M. Selection of Die Material and Its Impact on the Multi-Material Extrusion of Bimetallic AZ31B-Ti6Al4V Components for Aeronautical Applications. Materials 2021, 4, 7568.
5. Negendanka, M.; Mueller, S.; Reimers, W. Co-extrusion of Mg–Al macrocomposites. *J. Mater. Process. Technol.* **2021**, 212, 1954–1962.
6. Gall, S.; Müller, S.; Reimers, W. Aluminum coating of magnesium hollow profiles by using the co-extrusion process. *Alum. Int. J.* **2009**, 85, 63–67.
7. Rai, R.; Tiwari, M.K.; Ivanov, D.; Dolgui, A. Machine learning in manufacturing and industry 4.0 applications. *Int. J. Prod. Res.* **2021**, 59, 4773–4778.
8. Dalzochio, J.; Kunst, R.; Pignaton, E.; Binotto, A.; Sanyal, S.; Favilla, J.; Barbosa, J. Machine learning and reasoning for predictive maintenance in Industry 4.0: Current status and challenges. *Comput. Ind.* **2020**, 123, 103298.
9. Vapnik, V. The Nature of Statistical Learning Theory; Springer: New York, NY, USA, **1995**.
10. Jović, S.; Radović, A.; Šarkoćević, Ž.; Petković, D.; Alizamir, M. Estimation of the laser cutting operating cost by support vector regression methodology. *Appl. Phys. A* 2016, 122, 798.
11. Rabiee, A.H.; Tahmasbi, V.; Qasemi, M. Experimental evaluation, modeling and sensitivity analysis of temperature and cutting force in bone micro-milling using support vector regression and EFAST methods. *Eng. Appl. Artif. Intell*. **2023**, 120, 105874.
12. Xu, C.; Yao, S.; Wang, G.; Wang, Y.; Xu, J. A prediction model of drilling force in CFRP internal chip removal hole drilling based on support vector regression. *Int. J. Adv. Manuf. Technol*. **2021**, 117, 1505–1516.
13. Benkedjouh, T.; Medjaher, K.; Zerhouni, N.; Rechak, S. Health assessment and life prediction of cutting tools based on support vector regression. *J. Intell. Manuf.* **2015**, 26, 213–223.
14. Rebello, C.M.; Martins, M.A.F.; Santana, D.D.; Rodrigues, A.E.; Loureiro, J.M.; Ribeiro, A.M.; Nogueira, I.B.R. From a Pareto Front to Pareto Regions: A Novel Standpoint for Multiobjective Optimization. *Mathematics* **2021**, 9, 3152.
15. Saaty, T.L. A scaling method for priorities in hierarchical structures. *J. Math. Psychol*. **1977**, 15, 234–281.
16. Ghaleb, A.M.; Kaid, H.; Alsamhan, A.; Mian, S.H.; Hidri, L. Hindawi Assessment and Comparison of Various MCDM Approaches in the Selection of Manufacturing Process. *Adv. Mater. Sci. Eng*. **2020**, 4039253.
17. Karbassi Yazdi, A.; Tan, Y.; Spulbar, C.; Birau, R.; Alfaro, J. An Approach for Supply Chain Management Contract Selection in the Oil and Gas Industry: Combination of Uncertainty and Multi-Criteria Decision-Making Methods. *Mathematics* **2022**, 10, 3230.
18. Rodríguez-Prieto, A.; Camacho, A.M.; Sebastián, M.A. Multi-criteria materials selection for extreme operating conditions base on a multi-objective analysis of irradiation embrittlement and hot cracking prediction models. *Int. J. Mech. Mater. Des.* **2018**, 14, 617–634.
19. Alrababah, S.A.A.; Gan, K.H. Effects of the Hybrid CRITIC–VIKOR Method on Product Aspect Ranking in Customer Reviews. *Appl. Sci.* **2023**, 13, 9176.
20. Kao, C. Weight determination for consistently ranking alternatives in multiple criteria decision analysis. *Appl. Math. Model*. **2010**, 34, 1779–1787.
21. Dev, S.; Aherwar, A.; Patnaik, A. Material Selection for Automotive Piston Component Using Entropy-VIKOR method. *Silicon* **2020**, 12 (4).
22. Fernández, D.; Rodríguez-Prieto, Á.; Camacho, A.M. Optimal Parameters Selection in Advanced Multi-Metallic Co-Extrusion Based on Independent MCDM Analytical Approaches and Numerical Simulation. *Mathematics* **2022**, 10, 4489.
23. Zavadskas, E.K.; Turskis, Z. A new additive ratio assessment (ARAS) method in multicriteria decision-making. *Technological and Economic Development of Economy* **2010**, 16 (2), pp 159-172.
24. Behzadian, M.; Otaghsara, S.K.; Yazdani, M.; Ignatius, J. A state-of the-art survey of TOPSIS applications. *Expert Syst. Appl.* **2012**, 39, pp.13051–13069.
25. Zavadskas, E.K.; Kaklauskas, A.; Peldschus, F.; Turskis, Z. Multi-attribute assessment of road design solutions by using the COPRAS method. *Balt. J. Road Bridge Eng.* **2007**, 2, pp.195–203.
26. Pant, S.; Kumar, A.; Ram, M.; Klochkov, Y.; Sharma, H.K. Consistency Indices in Analytic Hierarchy Process: A Review. *Mathematics* **2022**, *10*, 1206.
27. Narayanamoorthy, S.; Annapoorani, V.; Kalaiselvan, S.; Kang, D. Hybrid Hesitant Fuzzy Multi-Criteria Decision Making Method: A Symmetric Analysis of the Selection of the Best Water Distribution System. *Symmetry* **2020**, 12, 2096.
28. Donachie, M.J. Titanium: A Technical Guide; ASM International: Novelty, OH, USA, **1988**
29. Avedesiam, M.; Baker, H. ASM Speciality Handbook: Magnesium and Magnesium Alloys; ASM International: Novelty, OH, USA, 1999.

30. Karmakar, D.; Muvvala, G.; Kumar, A. High-temperature abrasive wear characteristics of H13 steel modified by laser remelting and cladded with Stellite 6 and Stellite 6/30% WC. *Surf. Coat. Technol.* **2021**, 422, 127498.
31. Li, D.; Zhu, Z.; Xiao, S.; Zhang, G.; Lu, Y. Plastic flow behavior based on thermal activation and dynamic constitutive equation of 25CrMo4 steel during impact compression. *Mater. Sci. Eng. A* **2017**, 707, 459–465.
32. Bhandarkar, L.; Behera, M.; Mohanty, P.; Sarangi, S. Experimental investigation and multi-objective optimization of process parameters during machining of AISI 52100 using high performance coated tools. *Measurement* **2021**, 172, 108842.
33. Bedekar, V.; Voothaluru, R.; Yu, D.; Wong, A.; Galindo-Nava, E.; Gorti, S.B.; An, K.; Hyde, R.S. Effect of nickel on the kinematic stability of retained austenite in carburized bearing steels—In-situ neutron diffraction and crystal plasticity modeling of uniaxial tension tests in AISI 8620, 4320 and 3310 steels. *Int. J. Plast*. **2020**, 131, 102748.
34. Peat, T.; Galloway, A.; Toumpis, A.; Steel, R.; Zhu, W.; Iqbal, N. Enhanced erosion performance of cold spray co-deposited AISI316 MMCs modified by friction stir processing. *Mater. Des*. **2017**, 120, 22–35.
35. Davis, J.R. ASM Speciality Handbook—Stainless Steels; ASM International: Novelty, OH, USA, **1999**.
36. Scientific Forming Technologies. DEFORM v11.2 User's Manual; Scientific Forming Technologies Corporation: Columbus, OH, USA, **2017**.
37. Li, W.; Zhao, G.; Ma, X.; Gao, J. Flow Stress Characteristics of AZ31B Magnesium Alloy Sheet at Elevated Temperatures. *Int. J. Appl. Phys. Math*. **2012**, 2, 83–88.
38. Wang, F.; Zhao, J.; Zhu, N.; Li, Z. A comparative study on Johnson—Cook constitutive modelling for Ti6Al4V alloy using automated ball indentation (ABI) technique. *J. Alloys Compd*. **2015**, 633, 220–228.
39. Zhang, C.; Zhao, G.; Li, T.; Guan, Y.; Chen, H.; Li, P. An Investigation of Die Wear Behavior during Aluminum Alloy 7075 Tube Extrusion. *J. Tribol*. **2012**, 135, 011602.
40. Li, T.; Zhao, G.; Zhang, C.; Guan, Y.; Sun, X.; Li, H. Effect of Process Parameters on Die Wear Behavior of Aluminum Alloy Rod Extrusion. *Mater. Manuf. Process*. **2013**, 28, 312–318.
41. Lepadatu, D.; Hambli, R.; Kobi, A.; Barreau, A. Statistical investigation of die wear in metal extrusion processes. *Int. J. Adv. Manuf. Technol*. **2005**, 28, 272–278.
42. García-Domínguez, A., Claver, J., Camacho, A.M. & Sebastián, M.A. Comparative analysis of extrusion processes by finite element analysis. *Procedia Engineering* **2015**; 100: 74-83.
43. Gisbert, C., Bernal, C. & Camacho, A.M. Improved analytical model for the calculation of forging forces during compression of bimetallic axial assemblies. *Procedia Engineering* **2015**; 132: 298-305.
44. Safari, M.; Rabiee, A.H.; Joudaki, J. Developing a Support Vector Regression (SVR) Model for Prediction of Main and Lateral Bending Angles in Laser Tube Bending Process. *Materials* **2023**, 16, 3251.
45. Opricovic, S.; Tzeng, G.H. Compromise solution by MCDM methods: A comparative analysis of VIKOR and TOPSIS. *Eur. J. Oper. Res*. **2004**, 156, 445–455.
46. Sasanka, C. T. ; Ravindra, K. Implementation of VIKOR Method for Selection of Magnesium Alloy to Suit Automotive Applications. *International Journal of Advanced Science and Technology* **2015**, Vol.83, 49–58.
47. Raschka, S.; Mirjalili, V. Python Machine Learning. Second Edition. Packt Publishing. Birminghan, UK. **2017**.